*Supporting Information for*

# Boron-Rich, Cytocompatible Block Copolymer Nanoparticles by Polymerization-Induced Self-Assembly

Lin-Chiang Sherlock Huang,[a,b,c,‡] Dao Le,[a,b,d,‡] I-Lun Hsiao,[e,f] Susanne Fritsch-Decker,[e] Christian Hald,[a,b] Su-Ching Huang,[g] Jen-Kun Chen,[g] Jih Ru Hwu,[c] Carsten Weiss,[e] Min-Hua Hsu,[h]* and Guillaume Delaittre[a,b,i]*

[a]Institute of Biological and Chemical Systems – Functional Molecular Systems (IBCS-FMS), Karlsruhe Institute of Technology (KIT), Hermann-von-Helmholtz-Platz 1, 76344 Eggenstein-Leopoldshafen, Germany
[b]Institute for Chemical Technology and Polymer Chemistry (ITCP), Karlsruhe Institute of Technology (KIT), Engesserstrasse 15, 76131 Karlsruhe, Germany
[c]Department of Chemistry, National Tsing Hua University, Hsinchu 30013, Taiwan
[d]Polymer Chemistry Team (ECP), Institut Parisien de Chimie Moléculaire (IPCM), Sorbonne Université and CNRS, UMR 8232, 4 Place Jussieu, 75005 Paris, France
[e]Institute of Biological and Chemical Systems – Biological Information Processing (IBCS-BIP), Karlsruhe Institute of Technology (KIT), Hermann-von-Helmholtz-Platz 1, 76344 Eggenstein-Leopoldshafen, Germany
[f]School of Food Safety, College of Nutrition, Taipei Medical University, No. 250, Wuxing St., Taipei 11031, Taiwan
[g]Institute of Biomedical Engineering and Nanomedicine, National Health Research Institutes, No.35, Keyan Rd., Zhunan Township, Miaoli County 35053, Taiwan
[h]Department of Chemistry, National Changhua University of Education, Changhua 50058, Taiwan
[i]Organic Functional Molecules, Organic Chemistry, University of Wuppertal, Gaußstrasse 20, 42119 Wuppertal, Germany

‡ These authors have contributed equally to this work.

Email: minghuahsu@cc.ncue.edu.tw; delaittre@uni-wuppertal.de

## Table of Contents



## Materials

4-(Hydroxymethyl)phenylboronic acid (abcr, 98%), pinacol (TCI, > 98.0%), magnesium sulfate ($MgSO_4$; VWR, ≥ 98.0%), methacrylic acid (Fisher, 99.5%), 1-ethyl-3-(3-dimethylaminopropyl) carbodiimide-hydrochloride (EDC·HCl; Roth, ≥ 99%), 4-(dimethylamino)pyridine (DMAP; Sigma Aldrich, ≥ 99%), 2-cyano-2-propyl benzodithioate (CPBD; Sigma Aldrich, > 97%), 4-cyano-4-(phenylcarbonothioylthio) pentanoic acid *N*-succinimidyl ester (NHS-CPBD; Sigma Aldrich), 3-aminobenzeneboronic acid (abcr,

97%), fluorescein *O*-methacrylate (FMA; Sigma Aldrich, 97%), tetrahydrofuran (THF; Sigma Aldrich, anhydrous ≥ 99.9%), dichloromethane (DCM; VWR, ≥ 99.5%), ethyl acetate (EtOAc; Roth, ≥ 99,5%), cyclohexane (VWR, ≥ 99.5%), *N*,*N*-dimethylacetamide (DMAc; VWR, ≥ 99.0%), 1,4-dioxane (Roth, ≥ 99.5%), diethyl ether ($Et_2O$; Roth, ≥ 99.5%), ethanol (EtOH; Acros, 99.8%), methanol (MeOH; Fisher, > 95%) were used without any further purification.

Oligo(ethylene glycol) methyl ether methacrylate $M_n$ = 300 g mol$^{-1}$ ($OEGMA_{300}$; Sigma-Aldrich, 98 %), oligo(ethylene glycol) methyl ether methacrylate $M_n$ = 500 g mol$^{-1}$ ($OEGMA_{500}$; Sigma-Aldrich, 98 %) were passed through a basic aluminum oxide column to remove inhibitor prior to polymerization. Azobisisobutyronitrile (AIBN; Sigma-Aldrich, 98 %) and 4,4'-azobis(4-cyanovaleric acid) (ACVA; Sigma-Aldrich, 98 %) were recrystallized from ethanol.

## Characterization

### Nuclear magnetic resonance (NMR) spectrometry

$^1$H NMR spectroscopy was performed on a Bruker NMR 500 spectrometer at 400 MHz. The samples were dissolved in deuterated solvent. The residual solvent signals were employed for chemical shift corrections.

### Size-exclusion chromatography (SEC)

Size-exclusion chromatography was performed on a Polymer Laboratories PL-SEC 50 Plus Integrated System comprising an autosampler, a PLgel 2.5 µm bead-size guard column (50 × 7.5 mm), followed by three PLgel 5 µm Mixed-C columns (300 × 7.5 mm), and a differential refractive index detector. *N,N*-Dimethylacetamide (DMAc) was employed as solvent with a flow rate of 1 mL min$^{-1}$ and a sample concentration of 2 g L$^{-1}$. The SEC system was calibrated with linear poly(methyl methacrylate) (PMMA) standards ranging from 700 to 2 × 10$^6$ g mol$^{-1}$. Prior injection the samples were filtered through PTFE membranes with a pore size of 0.2 µm.

### Dynamic light scattering (DLS)

DLS measurements were performed on a Zetasizer Nano ZS (Malvern). Nanoparticles obtained from PISA were diluted in water to a concentration of 1 mg mL$^{-1}$ and were not filtered prior to the measurements. Experiments were performed with 12 readouts of 3 independent measurements for each sample. To study the stability of nanoparticles in cell culture media, the stock solutions of nanoparticles were firstly filtered through a 0.22 µm syringe filter for sterilization. Fluorescence spectroscopy was used to quantify the concentration after filtration. Then, suspensions were diluted to 100 µg mL$^{-1}$ in DMEM 10% FBS or Medium 200/LSGS. The size was measured immediately (0 h) or after 24 h of incubation at 37 °C.

## Transmission electron microscopy (TEM)

TEM observations were carried out on a Zeiss EM 109T instrument operated at 80 kV. The polymerization reaction mixtures were diluted in water to a concentration of 1 mg $mL^{-1}$. 10 µL of uranyl acetate solution (1 wt%) were then mixed with 1 mL of this particle solution. A drop of 6 µL of the solution was placed on a copper grid for 20 seconds and then blotted using filter paper to remove excess solution.

## Electrospray ionization mass spectrometry (ESI-MS)

Spectra were recorded on an LXQ mass spectrometer (ThermoFisher Scientific) equipped with an atmospheric pressure ionization source operating in the nebulizer assisted electrospray mode. The instrument was calibrated in the *m*/*z* range 195−1822 using a standard mixture containing caffeine, Met-Arg-Phe-Ala acetate (MRFA), and a mixture of fluorinated phosphazenes (Ultramark 1621) (all from Aldrich). A constant spray voltage of 4.5 kV was used. Nitrogen at a dimensionless sweep gas flow rate of 2 (approximately 3 L $min^{-1}$) and a dimensionless sheath gas flow rate of 5 (approximately 0.5 L $min^{-1}$) was applied. The capillary voltage, the tube lens offset voltage, and the capillary temperatures were set to 34 V, 90 V, and 275 °C, respectively. The samples were dissolved at a concentration of 0.1 mg $mL^{-1}$ in a mixture of DCM and MeOH (1:3) containing sodium trifluoroacetic acid (0.14 µg $L^{-1}$).

## Fluorescence spectroscopy

Fluorescence measurements were carried out on a Varian Cary Eclipse spectrometer with an excitation slit width of 5 nm, a resolution of 0.5 nm, and a scan rate of 30 nm $min^{-1}$ in water at 25 °C. The excitation wavelength for FMA is 490 nm. The analytes were dissolved in water with a concentration of 0.1 mg $mL^{-1}$.

## Synthesis

### Synthesis of 4-pinacolboronylbenzyl methacrylate PBBMA

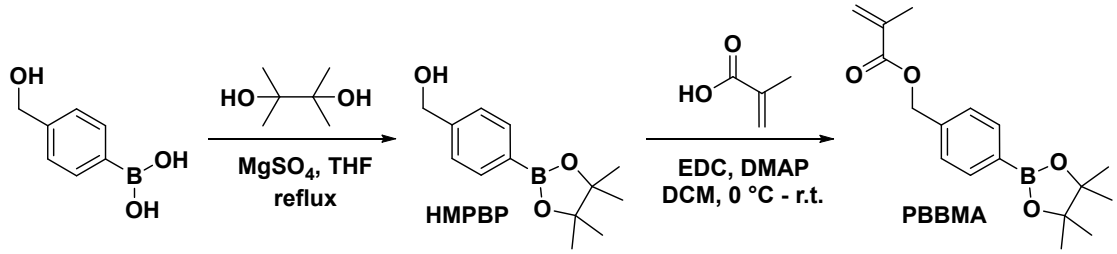


4-(Hydroxymethyl)phenylboronic acid (1.00 g, 6.58 mmol, 1 eq.), pinacol (0.934 g, 7.90 mmol, 1.2 eq.), and magnesium sulfate (1.20 g, in excess) were dissolved in 35 ml THF and stirred over night at 50 °C. The reaction progress was followed by thin layer chromatography. Magnesium sulfate was filtered off and solvent was evaporated under reduced pressure. The crude product was purified by flash chromatography with cyclohexane:EtOAc (4:1) as an eluent. Evaporation of combined fractions and drying under reduced pressure resulted in hydroxylmethylphenylboronic pinacol ester (**HMPBP**) as a white solid (1.24 g, 81 %).

**HMPBP** (1.24 g, 5.31 mmol, 1.5 eq.), methacrylic acid (0.335 g, 3.89 mmol, 1 eq.), and DMAP (0.0713 g, 0.584 mmol, 0.15 eq.) were dissolved in dry DCM (20 mL). The solution was cooled to 0 °C. EDC·HCl (1.87 g, 9.74 mmol, 2.5 eq.) in dry DCM (30 mL) was added dropwise into the mixture over the course of 1 h. After the addition the ice bath was removed, and the reaction mixture was stirred at room temperature overnight. The reaction mixture was then washed thrice with water (50 mL). The organic layer was dried over $Na_2SO_4$ and DCM was removed under reduced pressure. The residue was purified by column chromatography using a 1:24 vol/vol EtOAc/cyclohexane mixture as eluent. **PBBMA** was obtained as a pale-yellow oil (1.01 g, 86 %).

**TLC** $R_f$ = 0.188 (developed in 1:24 vol/vol EtOAc/cyclohexane)

**$^1$H NMR** (400 MHz, $CDCl_3$, ppm): $\delta$ 7.81 (d, J = 8.1 Hz, 2H), 7.37 (d, J = 8.2 Hz, 2H), 6.16 (s, 1H), 5.58 (s, 1H), 5.21(s, 2H), 1.34 (s, 12H).

**$^{13}$C NMR** (100 MHz, $CDCl_3$, ppm): $\delta$ 167.19 (C=O), 139.13 (C=), 136.21 (2CC, $C_6H_4$), 135.00 (2CH, $C_6H_4$), 127.15 (2CH, $C_6H_4$), 125.84 ($CH_2$=), 83.85 ($CH_2$), 66.29 ($CH_2$OC=O), 24.86 ($CH_3$), 18.34($CH_3$).

**$^{11}$B NMR** (100 MHz, $CDCl_3$, ppm): $\delta$ 31.0.

**ESI-MS** (*m/z*): $[M + Na]^+$ calc. for $C_{17}H_{23}BO_4$, 325.160; found, 325.158.

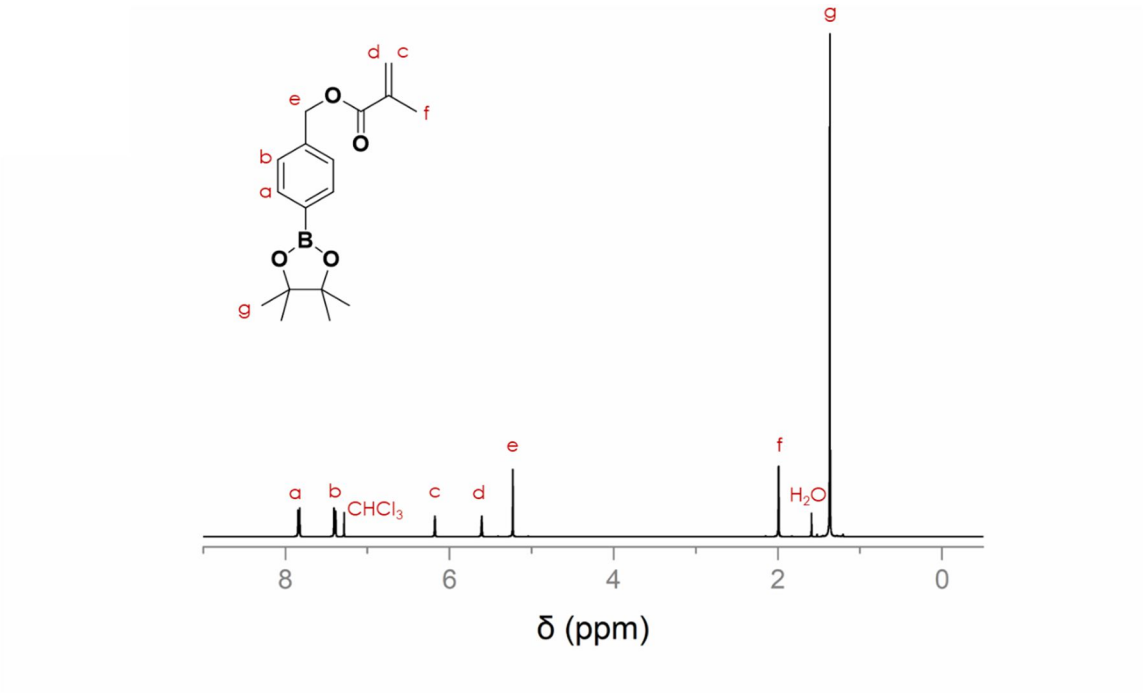


**Figure S1.** $^{1}H$ NMR spectrum of **PBBMA**; solvent: $CDCl_3$.

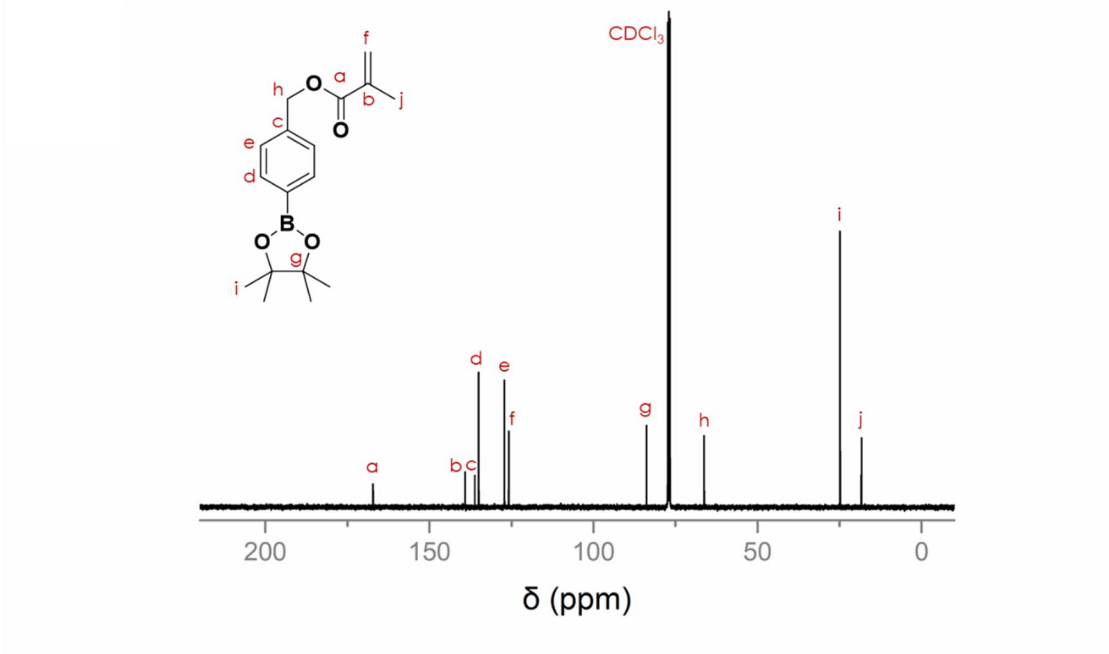


**Figure S2.** $^{13}C$ NMR spectrum of **PBBMA**; solvent: $CDCl_3$.

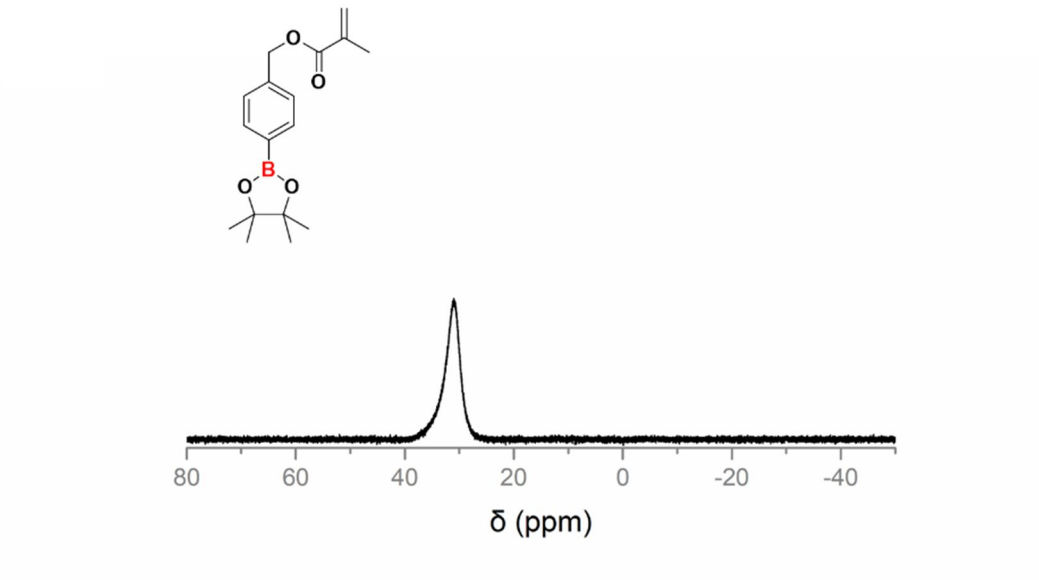


**Figure S3.** $^{11}B$ NMR spectrum of **PBBMA**; solvent: $CDCl_3$.

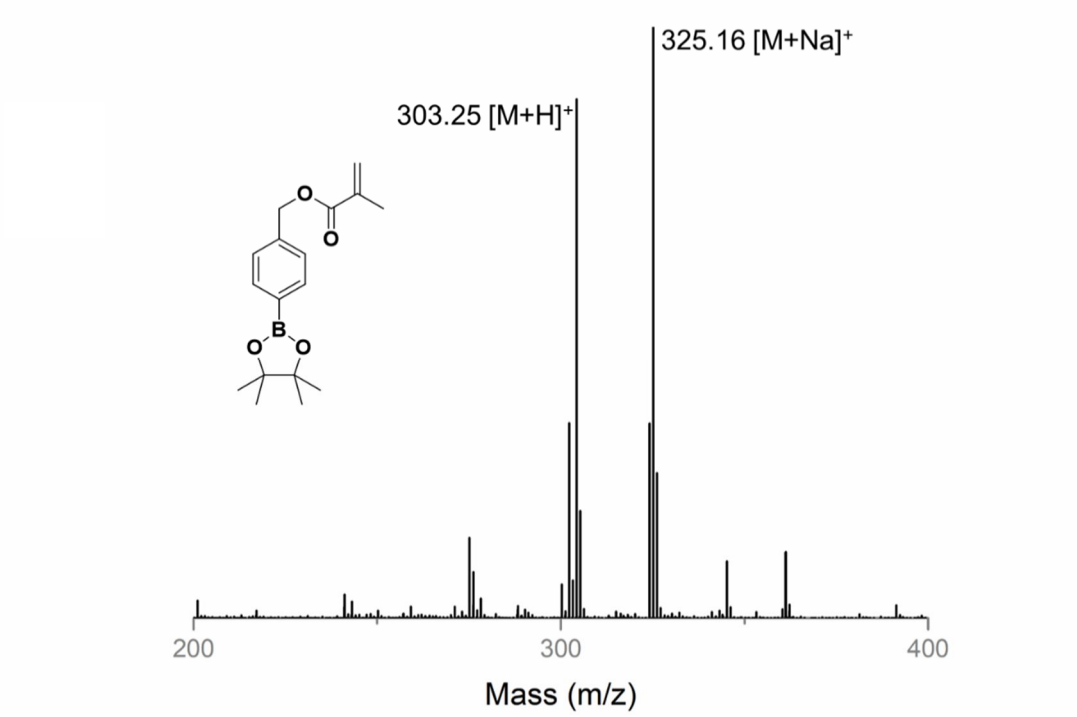


**Figure S4.** ESI-MS spectrum of **PBBMA**. *Theoretical: 303.18 $[M+H]^+$, 325.16 $[M+Na]^+$.*

**Solution RAFT Polymerization of PBBMA**

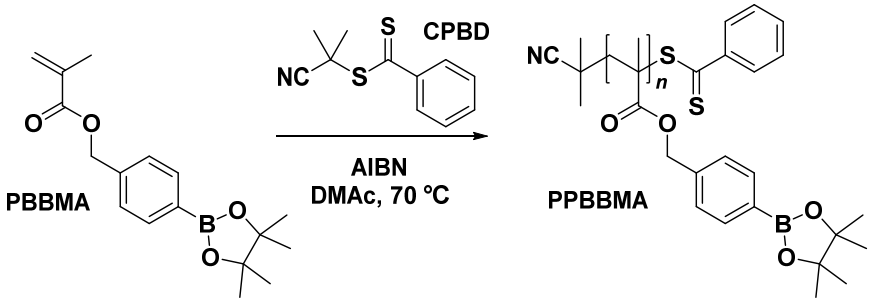


The RAFT polymerization kinetic were conducted at either 0.3M or 0.6 M of **PBBMA**, with $DP_{th}$ ([**PPBMA**]/[CPBD]) equal to 100, 200, and 400. In a typical experiment, **PBBMA**, CPBD (5.3 mg, 0.0145 mmol, 1 eq.), AIBN (1.2 mg, 7.30 µmol, 0.2 eq.), and DMAc were mixed in a flask. This solution was then split into several 1 mL sealable vials. The solutions were deoxygenated by bubbling with nitrogen for 15 min. The vials were placed in a preheated reaction block at 70 °C. Reaction vials were removed at predetermined time intervals to determine monomer conversion by $^1$H NMR spectroscopy, and molar mass and dispersity (*Đ*) of the resulting polymer by SEC.

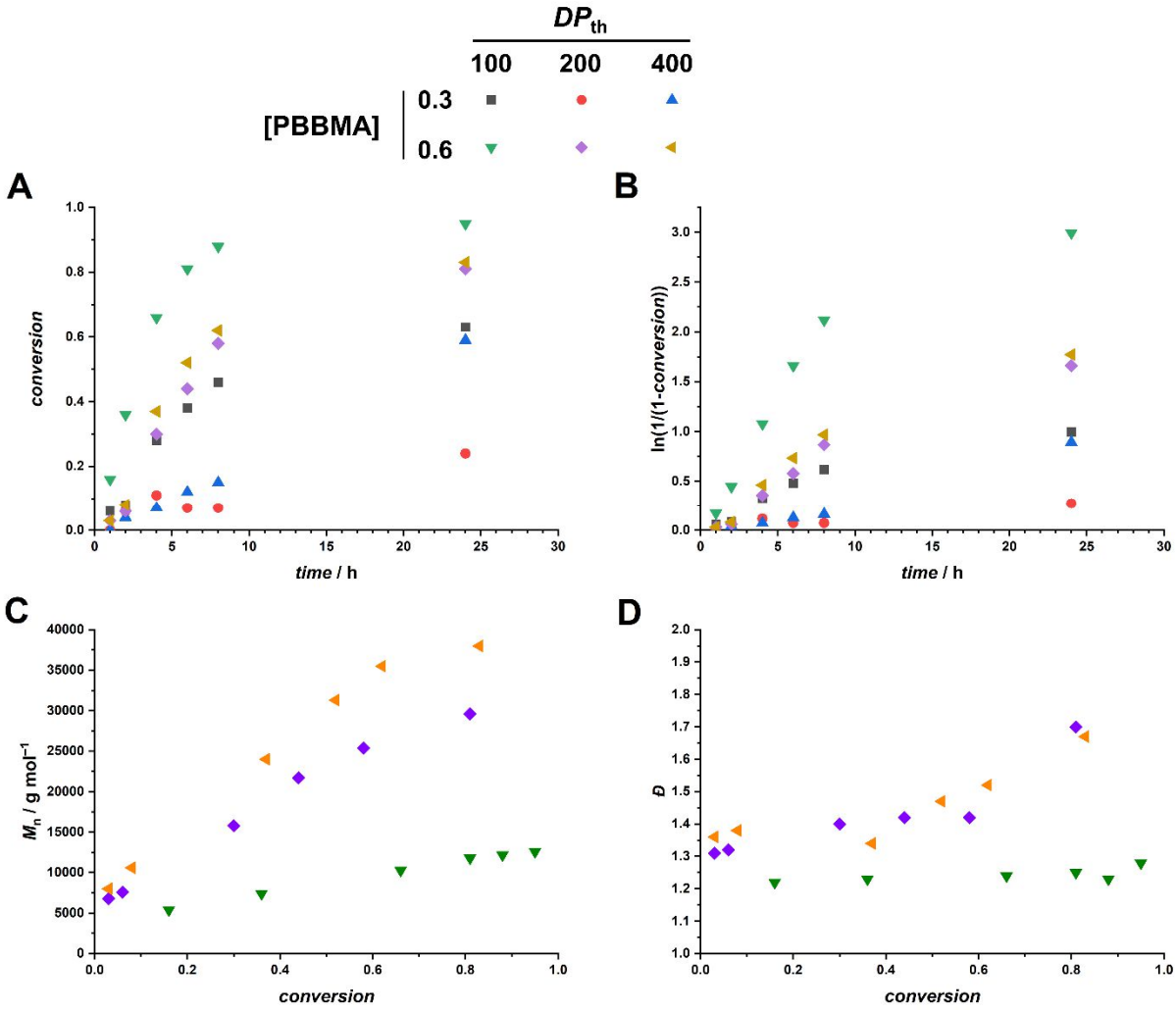


**Figure S5**. (A) Conversion *vs* time plot, (B) Pseudo first-order kinetic plot, (C) $M_n$ vs conversion plot, and (D) dispersity (*Đ*) *vs* conversion plot for the RAFT polymerization of **PBBMA** in DMAc at 70 °C, at various monomer concentrations and $DP_{th}$.

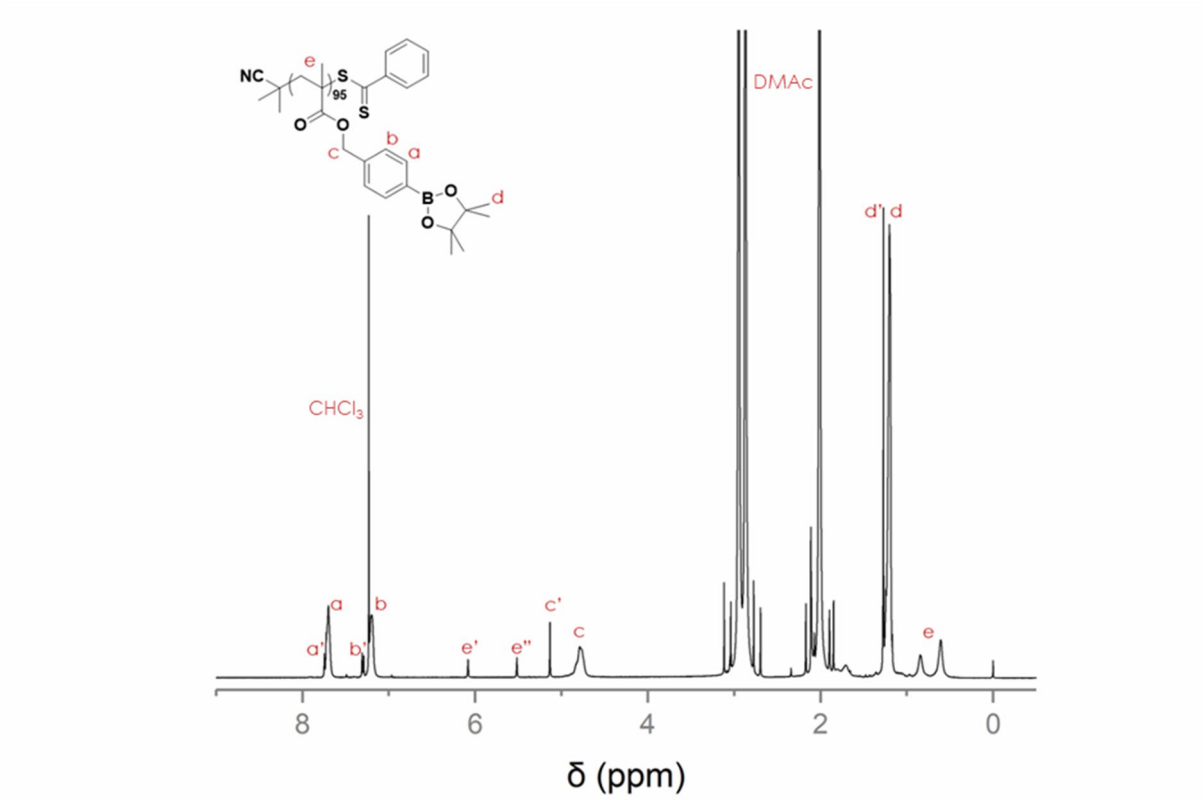


**Figure S6.** $^{1}$H NMR spectrum of raw **PPBBMA** typically employed for monomer conversion determination (here, [**PBBMA**] = 0.6 M, $DP_{th}$ = 100, 24 h); solvent: $CDCl_3$. *Signals a', b', c', d' and e' originate from residual monomer.*

## Synthesis of POEGMA macroCTAs

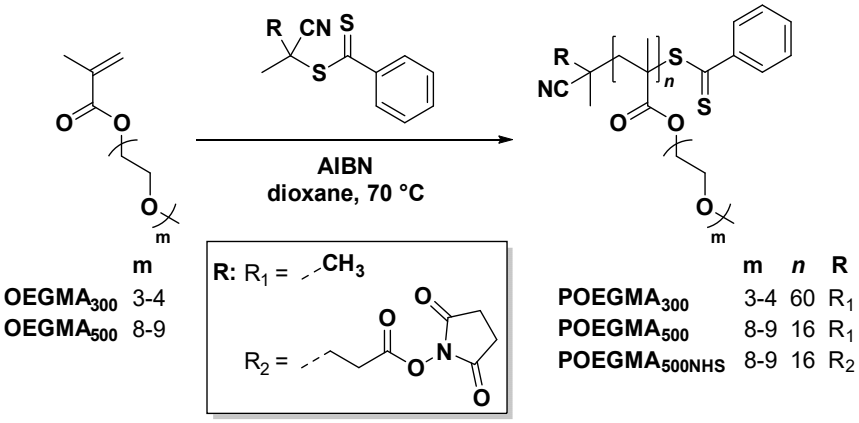


A round bottle flask was loaded with a stirring bar, $OEGMA_{300}$ (100 eq.) or $OEGMA_{500}$ (22 eq.) (100 eq. or 22 eq.), CPBD (for **$POEGMA_{300}$** and **$POEGMA_{500}$**) or NHS-CPBD (for **$POEGMA_{500NHS}$**) (1 eq.), AIBN (0.1 eq.), and 1,4-dioxane. The flask was sealed with a septum. The reaction mixture was deoxygenated by bubbling nitrogen for 30 minutes and the flask was subsequently placed in an oil bath pre-heated to 70 °C. After 3.5 h, polymerization was stopped by cooling to room temperature and opening the flask to air. Dioxane was removed under reduced pressure. The residue was dissolved in a small amount of

DCM. The polymer was precipitated three times into cold diethyl ether and obtained as a fuchsia oil after drying under vacuum.

**Table S1.** Structure and characteristics of macroCTA agents used in this study.

| Name | Structure | $M_{n,NMR}$[a] g mol$^{-1}$ | $Đ_{SEC}$ |
|---|---|---|---|
| **POEGMA$_{300}$** | 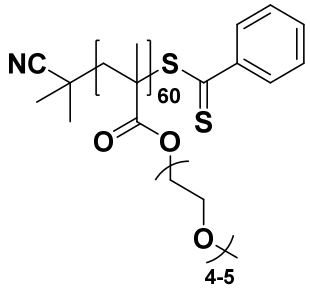 | 17620 | 1.15 |
| **POEGMA$_{500}$** | 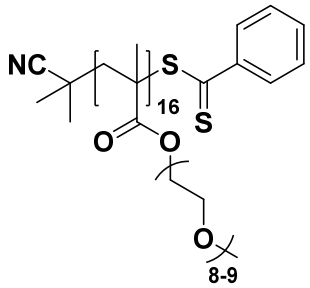 | 8220 | 1.15 |
| **POEGMA$_{500NHS}$** | 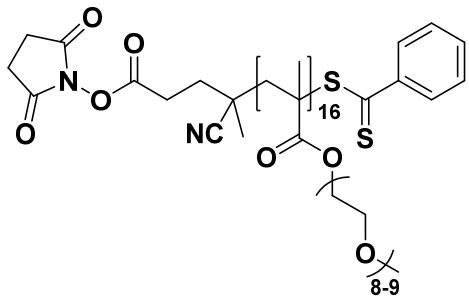 | 8370 | 1.19 |

[a]*calculations based on signals of phenyl end group and methylene group in alpha of the ester of repeating units after purification.*

## Polymerization-induced self-assembly (PISA) experiments

*Emulsion **PBBMA** RAFTPISA with **POEGMA$_{500}$***

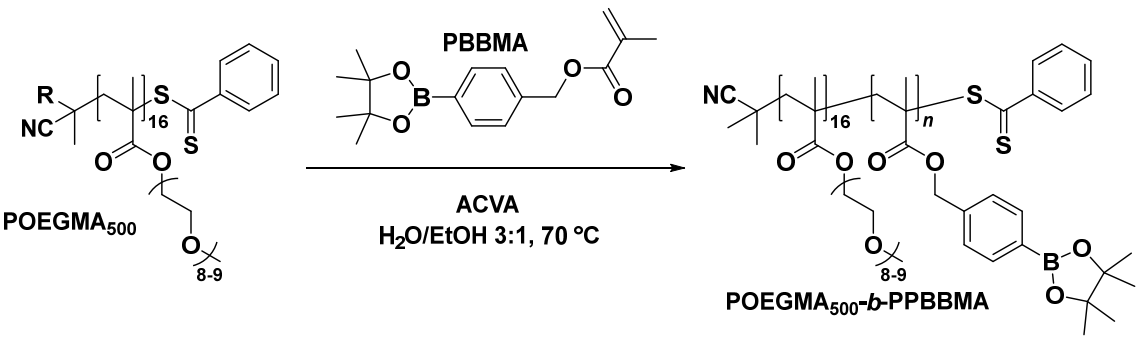


For $DP_{th}$ = 100, **PBBMA** (235.7 mg, 0.78 mmol), **POEGMA$_{500}$** (64.1 mg, 0.0078 mmol), 157.1 µL of ACVA (0.44 mg, 0.0016 mmol) stock solution (5.6 mg in 2 mL ethanol), and water/ethanol mixture (3:1 v/v, 0.793 mL) were added in a flask. The solution was deoxygenated by bubbling with $N_2$ for 20 minutes and the flask was then placed in an oil bath preheated to 70 °C to start the reaction. After a specific time, the flask was cooled down and exposed to air to stop the reaction. The mixture was analyzed with $^1$H NMR spectroscopy for monomer conversion determination, as well as with SEC for evaluation of the molar mass distribution.

**Table S2.** Conditions and characterization results for polymers and nanoparticles synthesized by emulsion RAFTPISA of **PBBMA** in water/ethanol using **POEGMA$_{500}$** as macroCTA*.*

| Entry | [POEGMA$_{500}$]/ [PBBMA]/ [ACVA] | Total solids content | Time | Conversion | *Z-average*[a] | *PdI*[a] | $M_{n,SEC}$[b] | *Đ*[b] | Visual observation |
|---|---|---|---|---|---|---|---|---|---|
| | | wt% | h | % | nm | | g mol$^{-1}$ | | |
| 1 | 100/1/0.2 | 10 | 2 | 60 | 50.2 | 0.046 | 27400 | 1.30 | small coagulum |
| 2 | 200/1/0.2 | 10 | 3 | - | - | - | 12800 | 1.30 | precipitation |
| 3 | 400/1/0.2 | 10 | 3 | - | - | - | 15000 | 1.24 | precipitation |
| 4 | 100/1/0.2 | 20 | 2 | 94 | 55.3 | 0.085 | 36200 | 1.68 | small coagulum |
| 5 | 200/1/0.2 | 20 | 3 | 25 | - | - | 17400 | 1.30 | precipitation |
| 6 | 400/1/0.2 | 20 | 3 | 16 | - | - | 28500 | 1.29 | precipitation |

Determined by [a]dynamic light scattering and [b]size-exclusion chromatography.

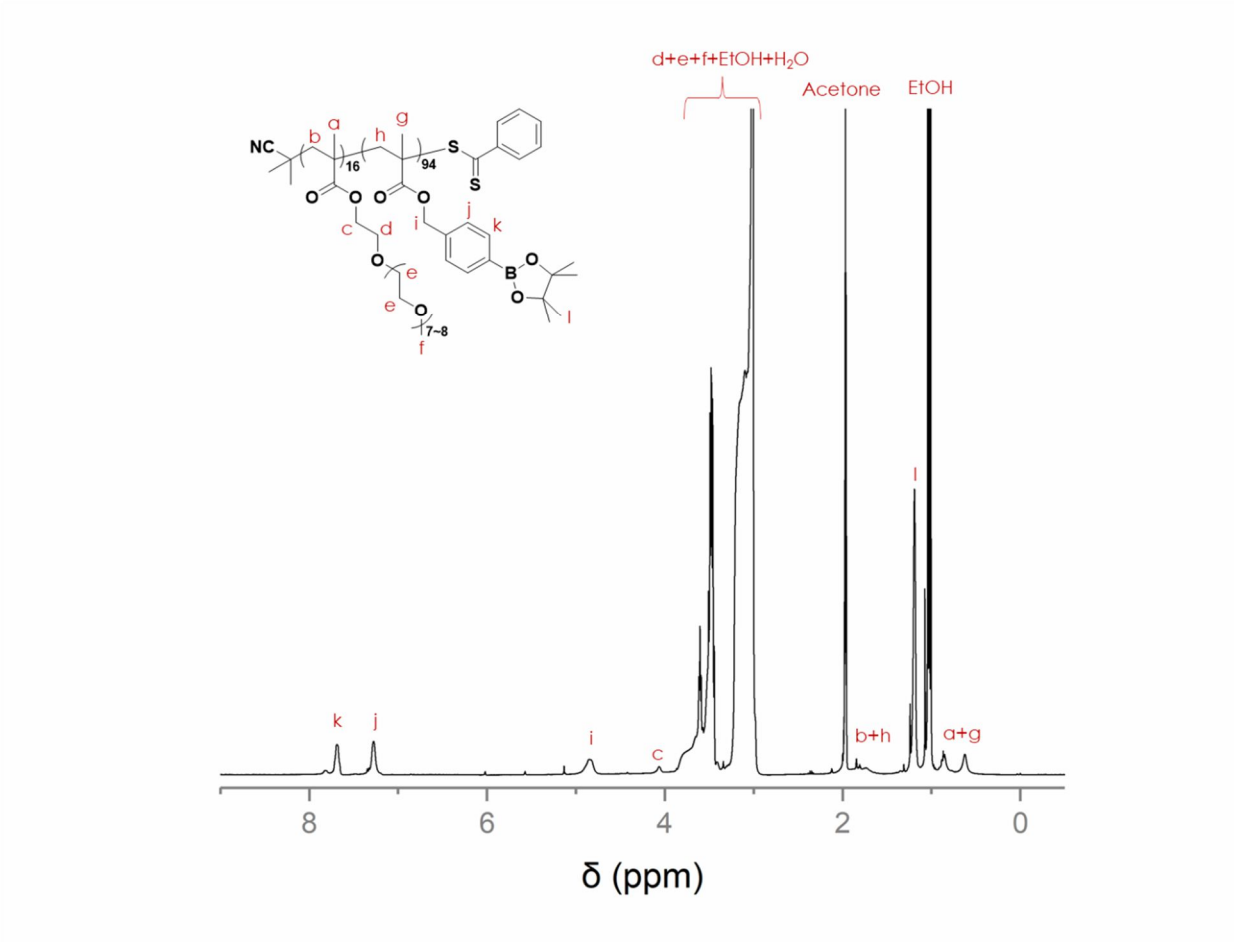


**Figure S7.** $^{1}$H NMR spectrum of raw block copolymer **POEGMA$_{500}$-*b*-PPBBMA** obtained by emulsion RAFTPISA at 20 wt% solids content after 2 h (Entry 4 in Table S2); solvent: acetone-*d6*.

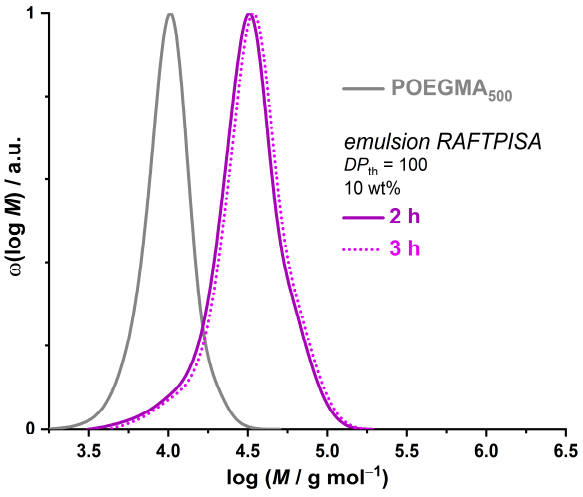


**Figure S8.** Size-exclusion chromatograms of polymers obtained by **PBBMA** emulsion RAFTPISA in water/ethanol 3:1 vol/vol at 70 °C with **POEGMA$_{500}$** at $DP_{th}$ 100, and 10 wt% solids content (Entry 1 from Table S2).

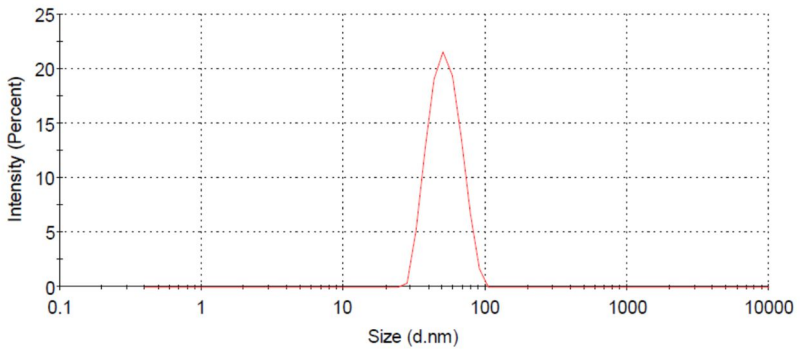


**Figure S9.** Intensity-average hydrodynamic diameter of nanoparticles obtained by **PBBMA** emulsion RAFTPISA in water/ethanol 3:1 vol/vol at 70 °C with **POEGMA$_{500}$** at $DP_{th}$ 100, and 10 wt% solids content, after 2 h (Entry 1 from Table S2).

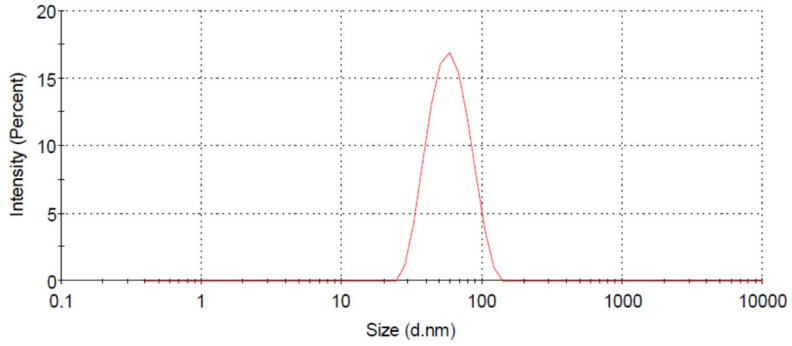


**Figure S10.** Intensity-average hydrodynamic diameter of nanoparticles obtained by **PBBMA** emulsion RAFTPISA in water/ethanol 3:1 vol/vol at 70 °C with **POEGMA$_{500}$** at $DP_{th}$ 100, and 20 wt% solids content, after 2 h (Entry 4 from Table S2).

*Dispersion RAFTPISA of **PBBMA***

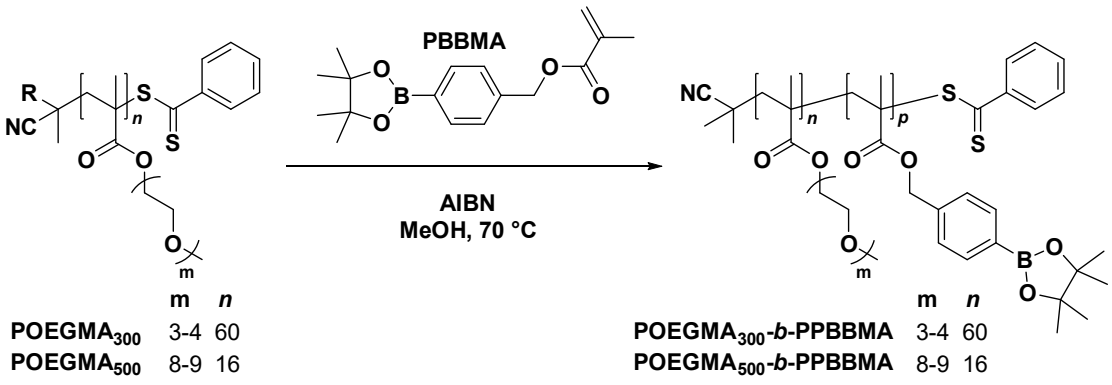


In a typical experiment, **PBBMA**, **POEGMA$_{300}$** or **POEGMA$_{500}$**, AIBN (15% w/v in methanol), and methanol (5 mL) were mixed in a flask. After complete dissolution, the mixture was equally split among several vials. The vials were sealed and then deoxygenated by bubbling with $N_2$ for 20 minutes. The polymerization mixtures were heated at 70 °C using a shaking thermomixer. Reaction was stopped at

predetermined time intervals to determine monomer conversion by $^1$H NMR spectroscopy, and molar mass and dispersity of resulting polymers by SEC.

- With **POEGMA$_{300}$**

**Table S3**. Conditions and characterization results for polymers and nanoparticles synthesized by **PPBMA** RAFTPISA using **POEGMA$_{300}$** as macroCTA.

| Entry | [POEGMA$_{300}$] /[PBBMA]/ [AIBN] | Total solids content | Time | Conversion | *Z-average*[a] | *PdI*[a] | $M_{n,SEC}$[b] | $Đ$[b] | Visual observation |
|---|---|---|---|---|---|---|---|---|---|
| | | wt% | h | % | nm | | g mol$^{-1}$ | | |
| 1 | 100/1/0.2 | 10 | 24 | 35 | 170.3 | 0.569 | - | - | translucent dispersion |
| 2 | 200/1/0.2 | 10 | 24 | 51 (gel) | 172.0 | 0.124 | - | - | gel |
| 3 | 400/1/0.2 | 10 | 24 | 56 (gel) | 231.1 | 0.184 | - | - | gel |
| 4 | 100/1/0.2 | 15 | 25 | 44 | 58.94 | 0.173 | 19300 | 1.40 | translucent dispersion |
| 5 | 200/1/0.2 | 15 | 24 | 46 (gel) | - | - | 27500 | 1.61 | gel |
| 6 | 400/1/0.2 | 15 | 24 | 71 (gel) | - | - | 52800 | 3.30 | gel |
| 7 | 100/1/0.5 | 15 | 25 | 94 | 60.06 | 0.168 | 31400 | 1.58 | milk |
| 8 | 200/1/0.5 | 15 | 24 | 68 | 105.3 | 0.181 | 43900 | 3.06 | dense milk |
| 9 | 100/1/0.5 | 30 | 24 | 99 | - | - | 27400 | 1.53 | gel |
| 10 | 200/1/0.5 | 30 | 25 | 97 | 511.0 | 0.275 | 42200 | 2.85 | gel and precipitation |
| 11 | 400/1/0.5 | 30 | 25 | 40 | 119.5 | 0.174 | 63400 | 5.73 | gel and precipitation |

Determined by [a]dynamic light scattering in water and [b]size-exclusion chromatography.

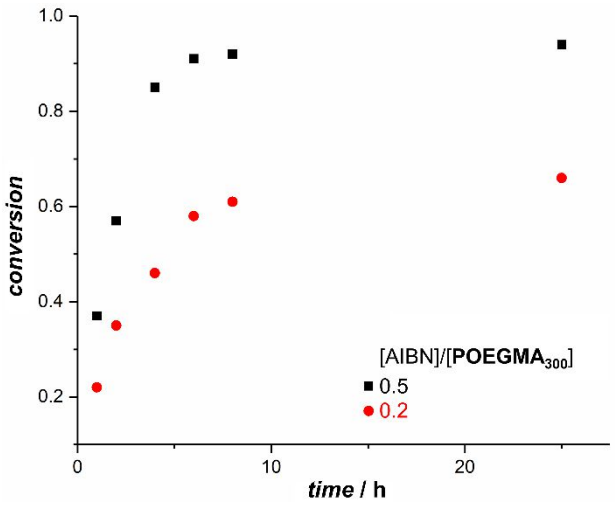


**Figure S11.** Conversion *vs* time plots for **PBBMA** dispersion RAFTPISA in methanol at 70 °C using **POEGMA$_{300}$** as macroCTA, at $DP_{th}$ = 100, 15 wt% solids content, for two distinct [AIBN]/[**POEGMA$_{300}$**] ratios.

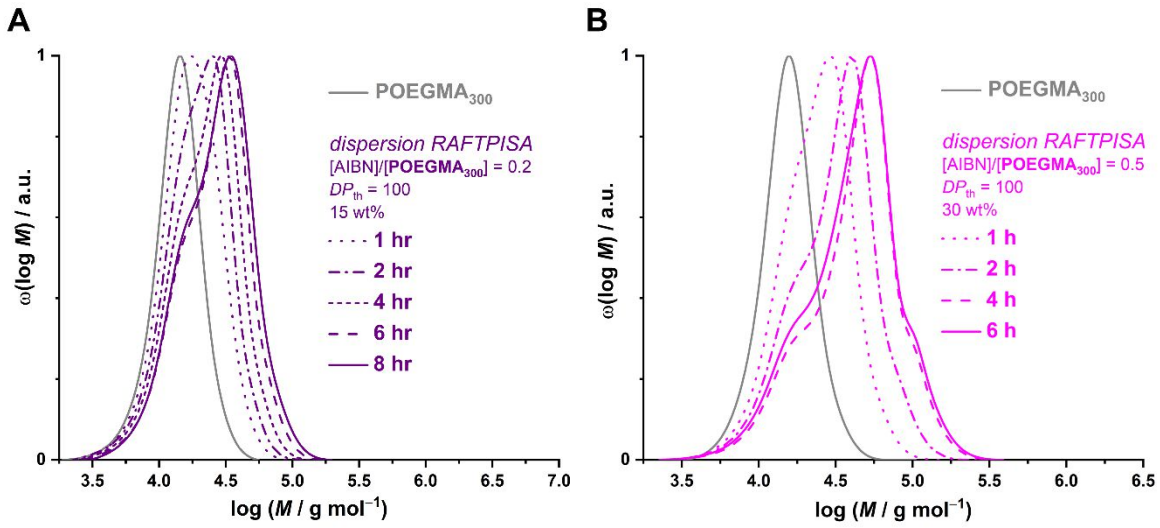


**Figure S12.** Size-exclusion chromatograms of **POEGMA$_{300}$** and **POEGMA$_{300}$-*b*-PPBBMA** block copolymers obtained by **PBBMA** dispersion RAFTPISA in methanol at 70 °C for $DP_{th}$ = 100, at various polymerization times at 15 wt% solids content and [AIBN]/[**POEGMA$_{300}$**] = 0.2 (A) and at 30 wt% solids content and [AIBN]/[**POEGMA$_{300}$**] = 0.5 (B).

**Table S4.** DLS results for nanoparticles synthesized by dispersion RAFTPISA with **POEGMA$_{300}$** according to conditions reported as Entry 7 in Table S3.

| reaction time | conversion | *Z-average* (MeOH) | *PdI* (MeOH) | *Z-average* (water) | *PdI* (water) |
|---|---|---|---|---|---|
| h | % | nm | | nm | |
| 1 | 37 | 28.92 | 0.172 | - | - |
| 4 | 85 | 48.15 | 0.012 | 52.91 | 0.068 |
| 6 | 91 | 51.97 | 0.01 | 54.48 | 0.053 |
| 8 | 92 | 56.47 | 0.099 | 60.88 | 0.115 |
| 25 | 94 | 56.17 | 0.089 | 60.06 | 0.168 |

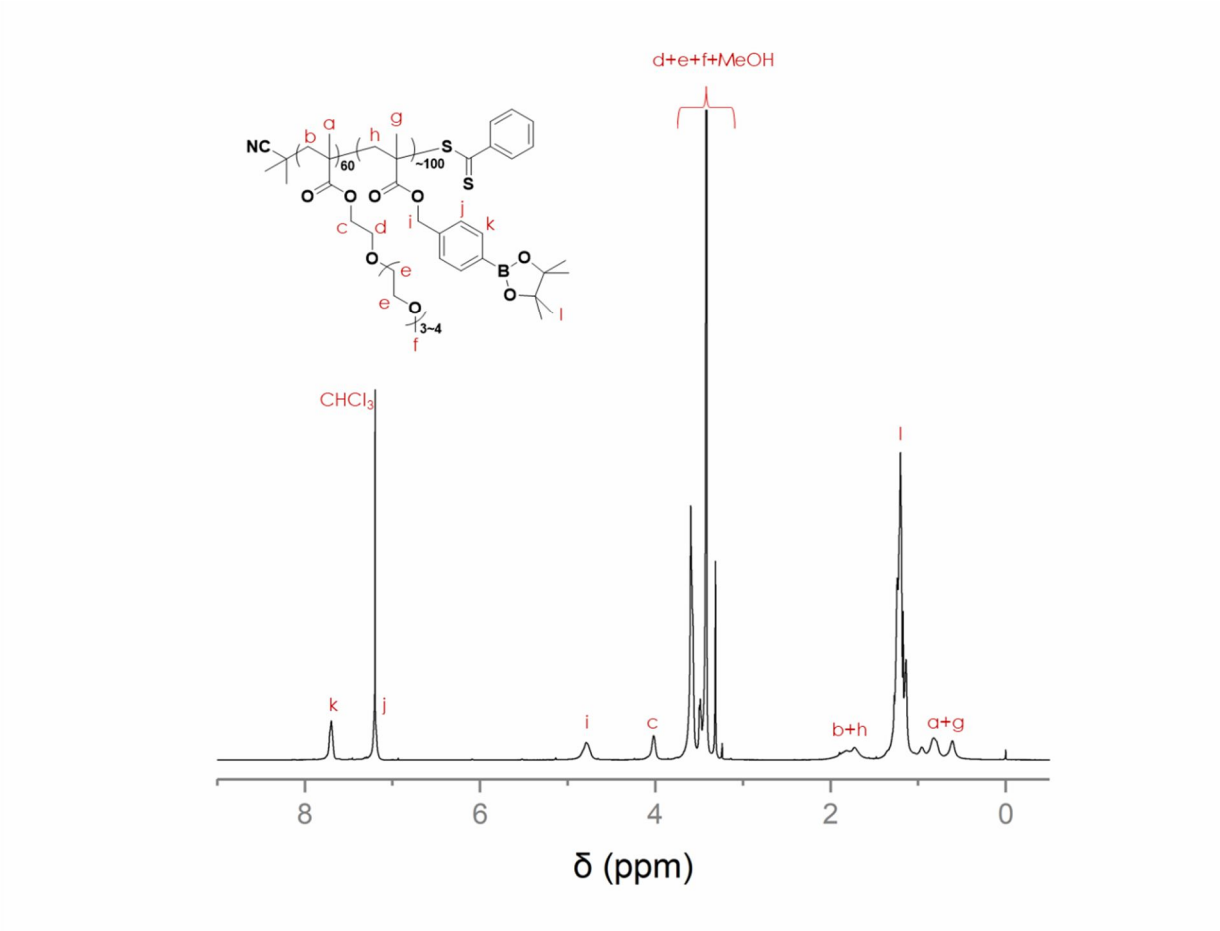


**Figure S13.** $^{1}$H NMR spectrum of block copolymer **POEGMA$_{300}$-*b*-PPBBMA** obtained by dispersion RAFTPISA at 15 wt% solids content and $DP_{th}$ = 100, with [AIBN]/[**POEGMA$_{300}$**] = 0.5, after 25 h (Entry 7 in Table S3); solvent: $CDCl_3$.

▪ With **POEGMA$_{500}$**

**Table S5.** Conditions and characterization results for polymers and nanoparticles synthesized by **PPBMA** RAFTPISA using **POEGMA$_{500}$** as macroCTA.

| Entry | [POEGMA$_{500}$] /[PBBMA]/ [AIBN] | Total solids content | Time | Conversion | *Z-average*[a] | *PdI*[a] | $M_{n,SEC}$[b] | *Đ*[b] | Visual observation |
|---|---|---|---|---|---|---|---|---|---|
| | | wt% | h | % | nm | | g mol$^{-1}$ | | |
| 1 | 100/1/0.5 | 15 | 8 | 92 | 144.5 | 0.220 | 26600 | 1.63 | milk |
| 2 | 100/1/0.5 | 20 | 8 | 97 | 124.2 | 0.218 | 32100 | 1.58 | gel |
| 3 | 100/1/0.5 | 30 | 4 | 96 | - | - | 34700 | 1.50 | gel |

Determined by [a]dynamic light scattering in water and [b]size-exclusion chromatography.

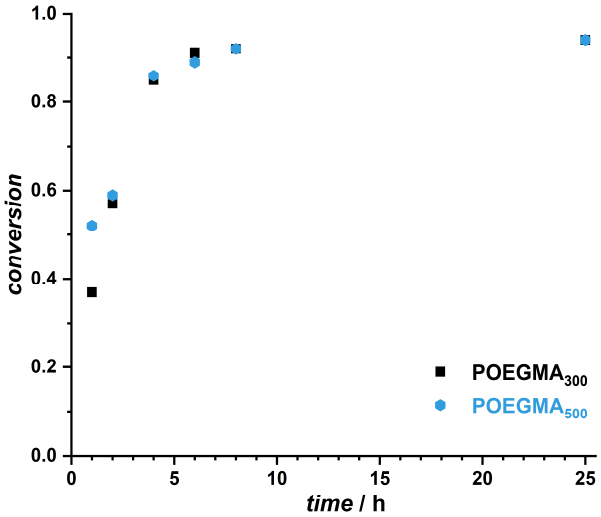


**Figure S14.** Conversion vs time plots for **PBBMA** dispersion RAFTPISA in methanol at 70 °C at $DP_{th}$ = 100, 15 wt% solids content, and [AIBN]/[**POEGMA**] = 0.5 for two distinct **POEGMA**s.

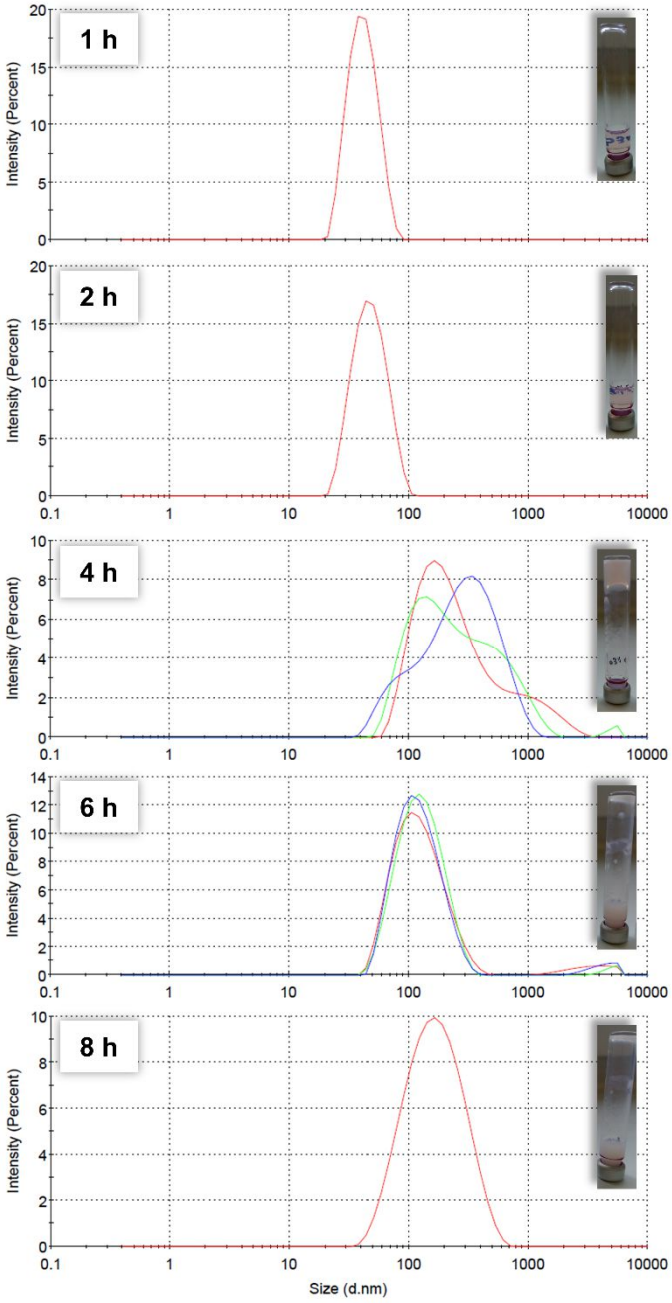


**Figure S15.** Evolution of the intensity-average hydrodynamic diameter distributions over polymerization for Entry 1 of Table S5. Insets: Photographs of corresponding samples following the tube inversion test.

**Table S6.** DLS results for nanoparticles synthesized by dispersion RAFTPISA with **POEGMA$_{500}$** according to conditions reported as Entry 1 in Table S5.

| reaction time | conversion | *Z-average* (water) | *PdI* (water) |
|---|---|---|---|
| h | % | nm | |
| 1 | 52 | 39.49 | 0.042 |
| 2 | 59 | 44.58 | 0.076 |
| 4 | 86 | 194.3 | 0.346 |
| 6 | 89 | 115.8 | 0.202 |
| 8 | 92 | 139.7 | 0.203 |
| 25 | 94 | 144.5 | 0.220 |

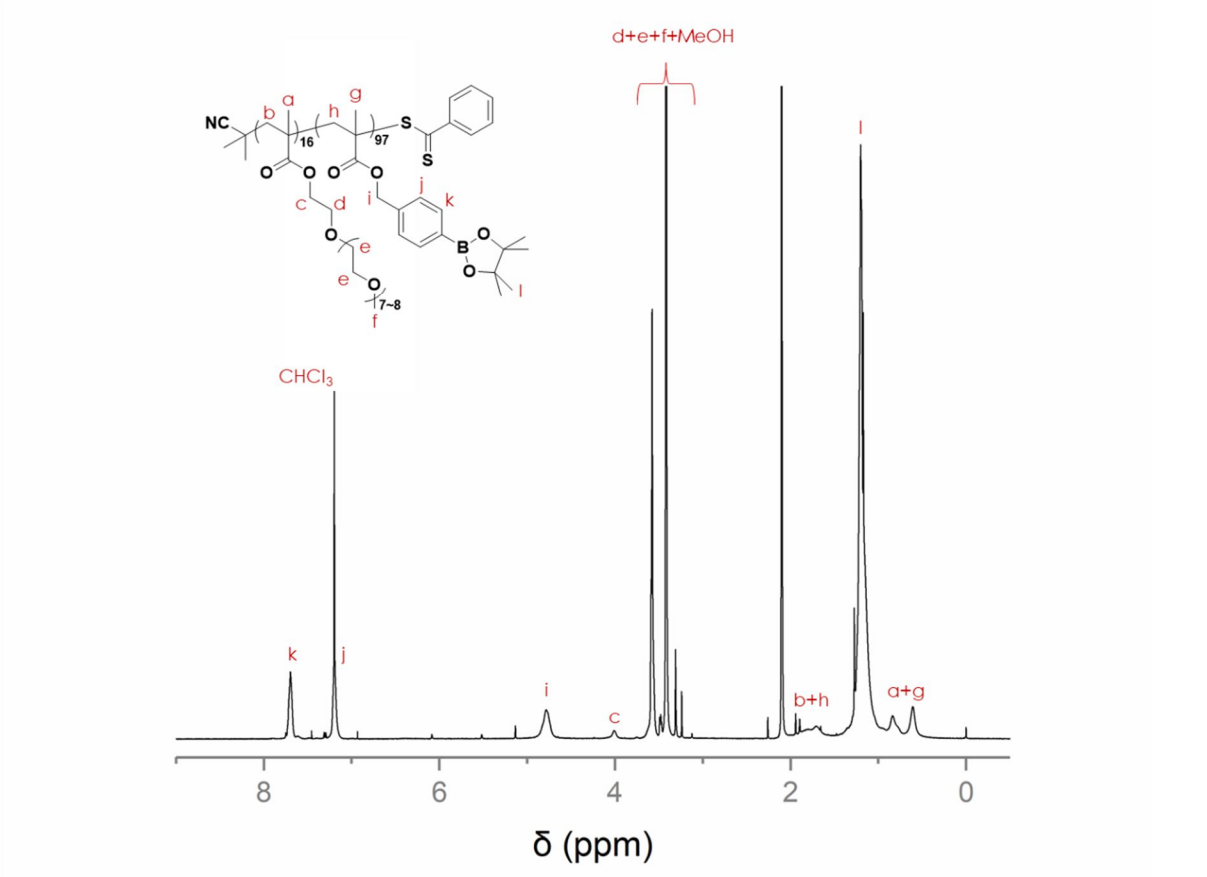


**Figure S16.** $^{1}$H NMR spectrum of block copolymer **POEGMA$_{500}$-*b*-PPBBMA** obtained by dispersion RAFTPISA at 15 wt% solids content and $DP_{th}$ = 100 after 25 h (Entry 1 in Table S5; solvent: $CDCl_3$.

▪ With **POEGMA$_{500}$** with additional pinacol

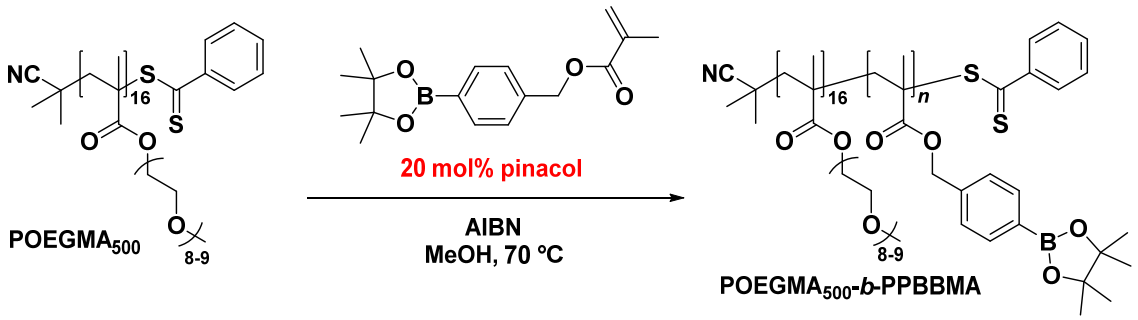


**PBBMA** (163.2 mg, 0.54 mmol), pinacol (12.8 mg, 0.11 mmol), **POEGMA$_{500}$** (47.5 mg, 0.0054 mmol), 63 µL of AIBN (0.44 mg, 0.0027 mmol) stock solution (3.5 mg in 2 mL of methanol), and methanol (5 mL) were added to a flask. After complete dissolution, the mixture was equally split among several vials. The vials were sealed and then deoxygenated by bubbling with $N_2$ for 20 minutes. The polymerization mixtures were heated at 70 °C using a shaking thermomixer. Reaction was stopped at predetermined time intervals to determine monomer conversion by $^1$H NMR spectroscopy, and molar mass and dispersity of resulting polymers by SEC.

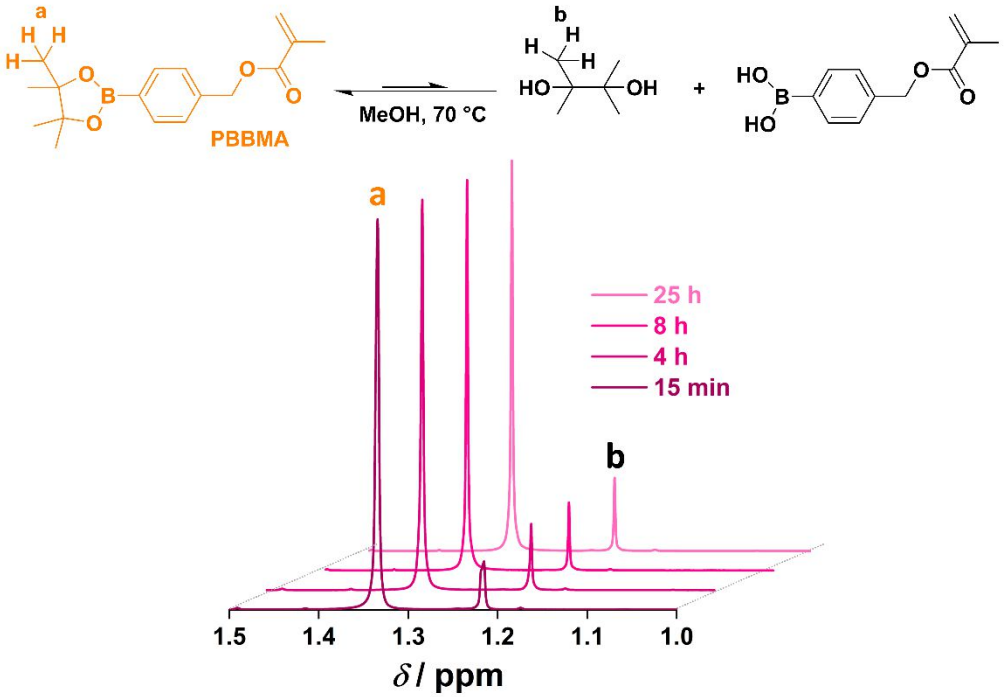


**Figure S17.** Selected region of the spectrum of PPBMA incubated in methanol at 70 °C for various periods of time; solvent: $CDCl_3$.

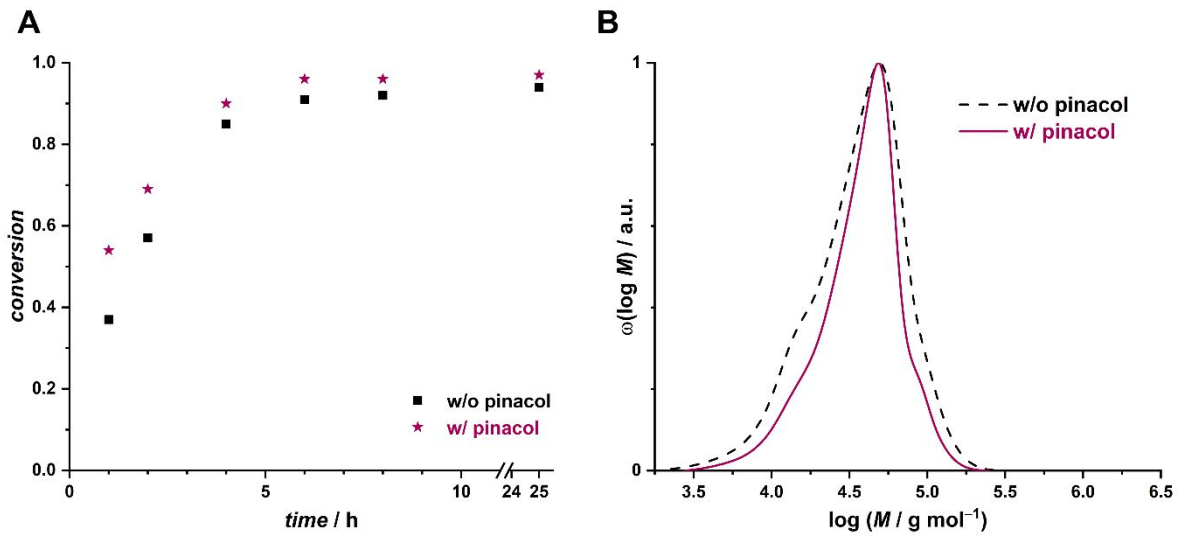


**Figure S18.** RAFTPISA of **PPBMA** with [AIBN]/[**POEGMA$_{500}$**] = 0.5, $DP_{th}$ = 100, 15 wt% solids content, with 20 mol% free pinacol (purple stars and line) or without pinacol (black squares and line, Entry 5 of Table S5). (A) Conversion *vs* time plots. (B) Size-exclusion chromatograms of obtained block copolymers **POEGMA$_{500}$-*b*-PPBBMA** after 8 h.

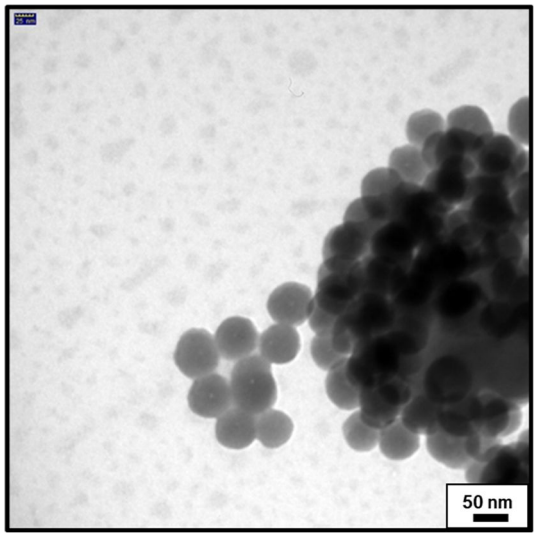


**Figure S19.** TEM images of block copolymers **POEGMA$_{500}$-*b*-PPBBMA** NPs obtained by **PBBMA** dispersion RAFTPISA in methanol at 70 °C, in the presence of 20 mol% of pinacol (with regards to **PBBMA**), for [AIBN]/[**POEGMA$_{500}$**] = 0.5, $DP_{th}$ = 100, 15 wt% solids content, at 25 h.

*Boron content calculations*

$$Boron\ content\ in\ copolymer\ (wt\%) = \frac{M_B * DP_{th} * conversion}{M_{PBBMA} * DP_{th} * conversion + M_{POEGMA}} * 100$$

$$Boron\ content\ in\ PISA\ solution\ (wt\%) = Boron\ content\ in\ copolymer \times solids\ content$$

- $M_B$ = 10.81 g mol$^{-1}$
- $M_{PBBMA}$ = 302.18 g mol$^{-1}$
- For best samples (see Conclusions in main text):
  - · $DP_{th}$ = 100;
  - · *conversion* = 0.94;
  - · solids content = 15 wt%;
  - · $M_{POEGMA}$ = 8220 g mol$^{-1}$ (Entry 4 in Table S2) or 17620 g mol$^{-1}$ (Entry 7 in Table S3).

*Synthesis of surface-functionalized and/or fluorescent POEGMA-b-PPBBMA nanoobjects*

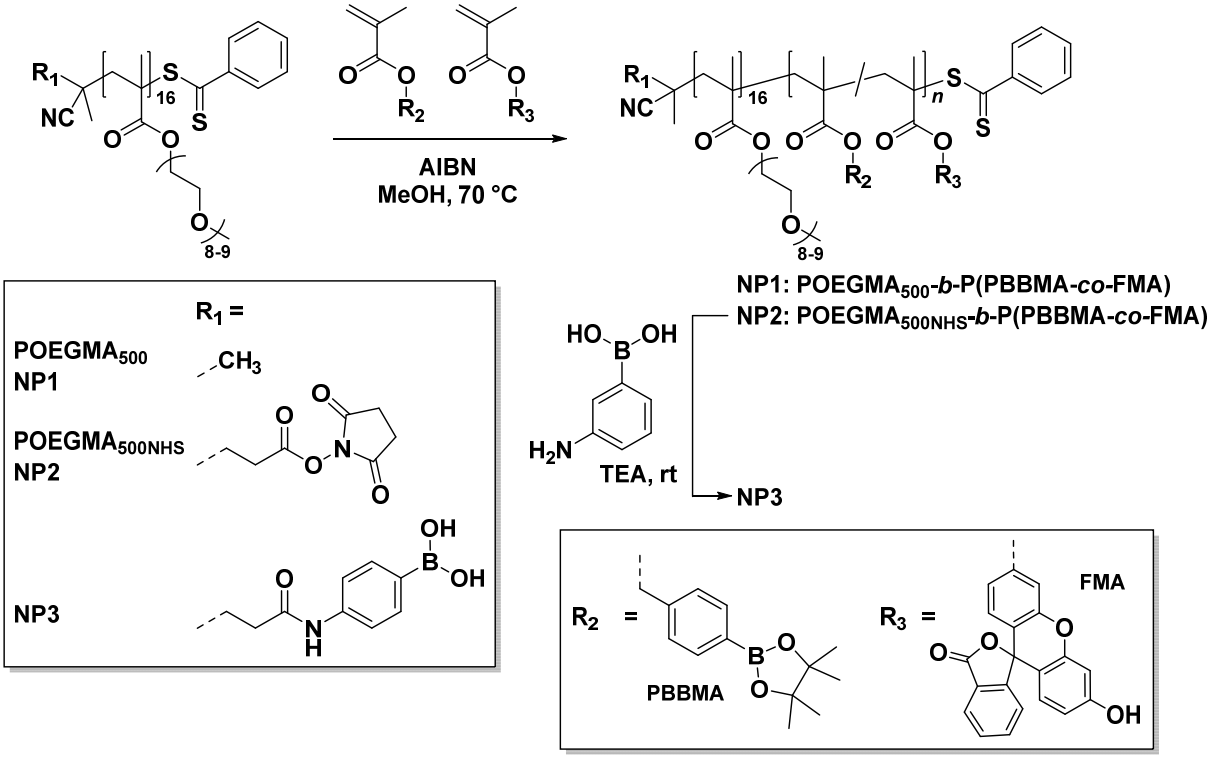


For the synthesis of **NP1** (with **POEGMA$_{500}$**, $DP_{th}$ = 100) and **NP2** (with **POEGMA$_{500NHS}$**, $DP_{th}$ = 50), a total solids content of 15 % wt was used: **PBBMA** (100 mg, 0.33 mmol), FMA (0.0066 mmol for **NP1**, and 0.013 mmol for **NP2**), **POEGMA$_{500}$** (0.0033 mmol) or **POEGMA$_{500NHS}$** (0.0066 mmol), AIBN (0.0017 mmol for **NP1** and 0.0033 mmol for **NP2**), methanol as the solvent, and a stir bar were added in a flask. The flask was sealed and the mixture deoxygenated by bubbling $N_2$ for 20 minutes. The flask was

subsequently placed in an oil bath preheated to 70 °C to start the reaction. After 6 hours, the reaction mixture was cooled down to room temperature. **NP2** were directly reacted with 3-aminobenzeneboronic acid to obtained **NP3**. **NP1** and **NP3** dispersions were dialyzed against methanol and then water, to remove unreacted monomers as well as 3-aminobenzeneboronic acid and free NHS, before being implemented for biocompatibility testing.

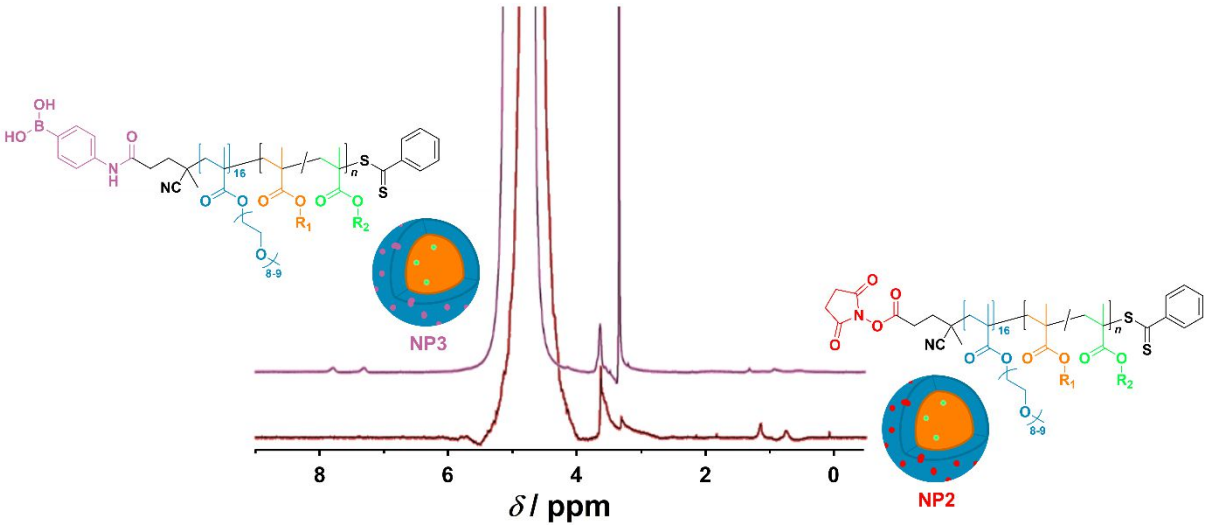


**Figure S20.** Overlay of NMR spectra of **NP2** (bottom, red) and **NP3** (top, purple) in MeOD.

**Table S7.** Hydrodynamic diameters obtained by DLS for NPs in cell media. *Note that PISA nanoparticles were stable in pure water over a period of several months.*

| Particles | DMEM/FCS | | | | M200/LSGS | | | |
|---|---|---|---|---|---|---|---|---|
| | 0 h | | 24 h | | 0 h | | 24 h | |
| | ***Z-av.*** nm | ***PdI*** | ***Z-av.*** nm | ***PdI*** | ***Z-av.*** nm | ***PdI*** | ***Z-av.*** nm | ***PdI*** |
| **NP1** | 60.7 | 0.14 | 81.1 | 0.16 | 66.7 | 0.09 | 1101 | 1.43 |
| **NP3** | 39.1 | 0.54 | 42.8 | 0.57 | 61.3 | 0.30 | 61.5 | 0.35 |
| PS-COOH[a] | 173.8 | 0.12 | 155.6 | 0.10 | 315.6 | 0.22 | 1291 | 0.56 |

[a]Data from our previous study.[1]

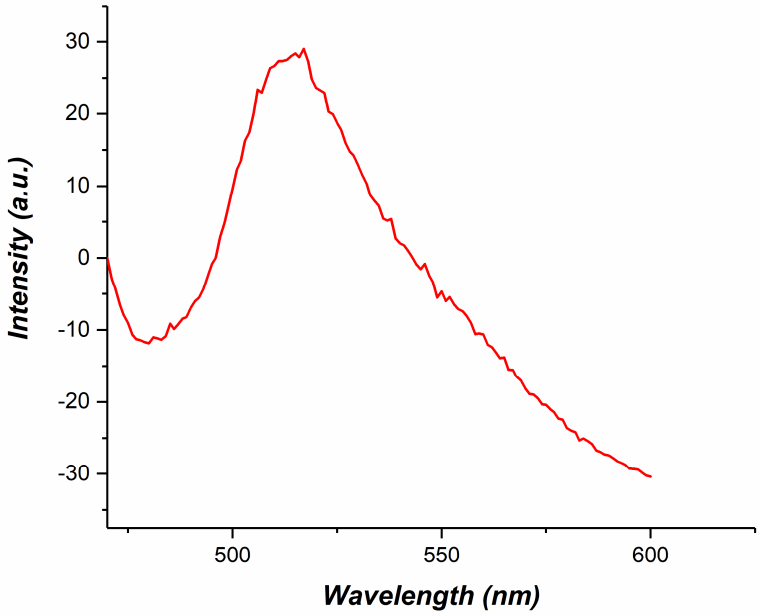


**Figure S21.** Emission spectrum of fluorescein-containing nanoparticles **NP1**; $\lambda_{ex}$ = 490 nm.

## Cytocompatibility of PISA Nanoparticles

### Cell culture

Murine macrophages (RAW 264.7) were cultured in Dulbecco's Modified Eagle's Medium (DMEM) medium supplemented with 10% fetal bovine serum (FBS), 1% L-glutamine and 1% penicillin/ streptomycin. Human umbilical vein endothelial cells (HUVEC) were cultured in Medium 200 supplemented with low serum growth supplement (LSGS) and 1% penicillin/streptomycin. Both cell lines were cultivated at 37 °C, 5% $CO_2$ and with 95% relative humidity.

### Cell viability determined by total cell number analysis

RAW 264.7 cells ($1.25 \times 10^4$ cells/well) and HUVEC ($1 \times 10^4$ cells/well) were cultured in 96-well plates. After 18 h of attachment, cells were incubated with NPs at 25, 50 and 100 µg/mL for 24 h. Then, Hoechst 33342 (final concentration: 0.3 µg $mL^{-1}$, 100 µL) was added and further incubated for 30 min. Finally, four images per well were captured using the automated fluorescence microscope IX81 (Olympus, Germany) with a 10-fold objective lens and DAPI cubic filters. Automated image analysis was conducted using the Olympus ScanR analysis software as previously described.[1] The total cell number was analyzed by the number of Hoechst-stained nuclei. Cell viability was expressed by (cell number in treatment group)/(cell number of unexposed control) × 100. Mean values ± SEM are given from two independent experiments.

## Cellular uptake and quantification

Cells were exposed to NPs as described above for the assessment of cell viability. Thereafter, cells were incubated with Hoechst 33342 for 30 min, all medium was discarded and 100 µL fresh medium was added. The NP uptake was detected by automated fluorescence microscopy employing GFP (ex. 457–487 nm; em. 502–538 nm) cubic filters (Olympus IX81, Olympus Corporation, Japan) with a 20-fold objective lens. Images were collected at exposure times of 4 and 500 ms. Outlines of cells and nuclei were automatically determined. To quantify the cellular uptake, the fluorescence images recorded in the GFP channel were analyzed by the ScanR software. The total number of cells per image were obtained by enumerating all nuclei as identified by edge detection in the DAPI channel. The mean fluorescence intensity per cell (MFI/cell) could be calculated with the following equation:

$$\text{MFI/cell} = (\text{total fluorescence})/(\text{total cell number})$$

Around 1000 RAW and 150 HUVEC cells were analyzed per treatment and the average cellular uptake (MFI/cell) was quantified. The brightness of NPs and PS-COOH NPs in water at 100 µg $mL^{-1}$ were measured at excitation wavelength of 485 ± 10 nm and emission wavelength of 530 ± 13 nm by using a fluorescence reader (MWG-Biotech AG, Ebersberg, Germany) (Figure S21). When quantifying the mean fluorescence intensity per cell, the normalized intensity of NPs was considered to compensate for the intensity differences among the three types of particles.

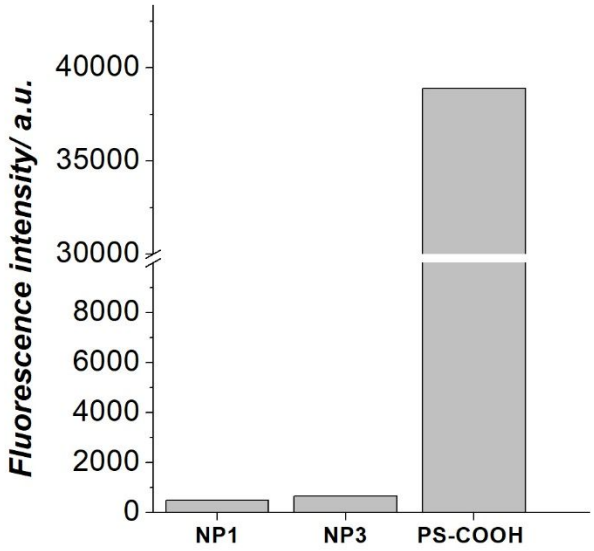


**Figure S22.** Fluorescence intensity of NPs were measured at 100 µg $mL^{-1}$ in water. Data was collected by a fluorometer under excitation wavelength 485 ± 10 nm and emission wavelength 530 ± 13 nm.

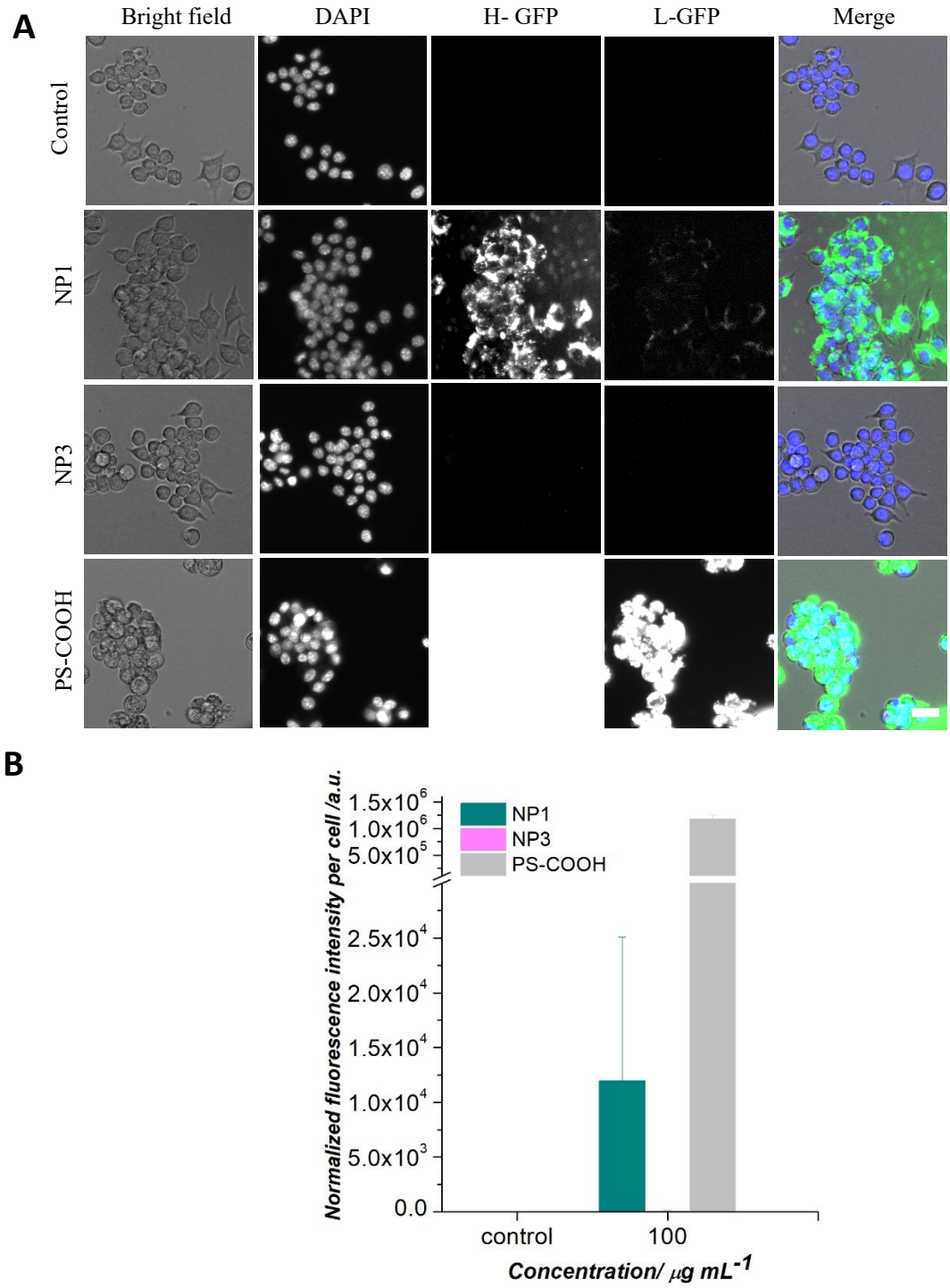


**Figure S23.** Cellular uptake of NPs in murine RAW264.7 macrophages. (A) *in vitro* uptake of NPs upon 24 h exposure of cells (100 µg $mL^{-1}$). Due to the 81 and 60 times higher fluorescence intensity of PS-COOH NPs compared to **NP1** and **NP3**, GFP signal was captured by automated fluorescence microscopy at either 4 ms (L-GFP) or 500 ms (H-GFP) exposure time. Images were overlapped using either H-GFP (**NP1** and **NP3**) or L-GFP (PS-COOH). Scale bar = 20 µm. (B) Quantitative uptake analysis depicting total fluorescence intensities (all using L-GFP images). The intrinsic intensity differences between each NPs were considered to normalize fluorescence intensity per cell. Error bars represent mean±SD. Note that due to the high fluorescence intensity of PS-COOH, over-saturated images at longer exposure time (H-GFP) are not depicted.

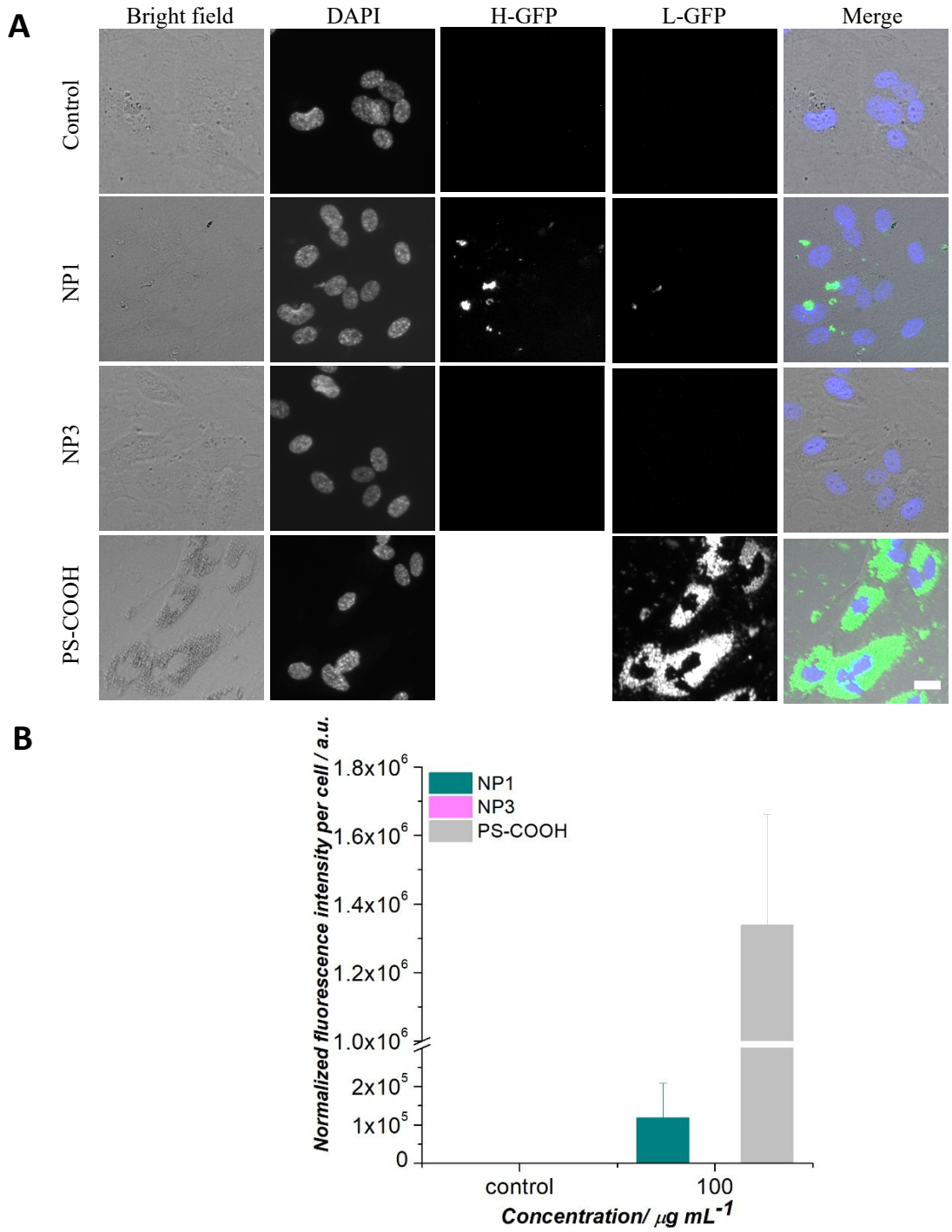


**Figure S24.** Cellular uptake of NPs in human umbilical vein endothelial cells (HUVECs). (A) *in vitro* uptake of NPs upon 24 h exposure of cells (100 µg $mL^{-1}$). Due to the 81 and 60 times higher fluorescence intensity of PS-COOH NPs compared to **NP1** and **NP3**, GFP signal was captured by automated fluorescence microscopy at either 4 ms (L-GFP) or 500 ms (H-GFP) exposure time. Images were overlapped using either H-GFP (**NP1** and **NP3**) or L-GFP (PS-COOH). Scale bar = 20 µm. (B) Quantitative uptake analysis depicting total fluorescence intensities (all using L-GFP images). The intrinsic intensity differences between each NPs were considered to normalize fluorescence intensity per cell. Error bars represent mean±SD. Note some large agglomerates in case of **NP1**, in accordance with the DLS data.

The relative *in vitro* doses (RIDs; Table S8) were calculated by the distorted grid transport simulator[2] and as described previously.[3]

**Table S8.** Calculation of the deposited cellular doses.

| Particles | Density of raw material [g/cm$^3$] | RID in DMEM/FCS [μg/cm$^2$] | RID in M200/LSGS [μg/cm$^2$] |
|---|---|---|---|
| NP1 | 1.15 | 6.1 | 21.8* |
| NP3 | 1.15 | 3.3 | 4.7 |
| PS-COOH | 1.1 | 7.5 | 21.9* |

*Note that for agglomerated NPs the effective density is lower and thus the deposited dose somewhat lower.

In the medium used to cultivate RAW macrophages, the calculated dose of **NP1** and PS-COOH is similar and in the case of **NP3** reduced by 50%. As in the culture medium of HUVECs NP1 and PS-COOH agglomerate, deposition is enhanced, yet again resulting in a similar dose for the two types of NPs. Therefore, the relative difference in uptake and toxicity are studied at similar cellular doses in case of RAW macrophages, demonstrating that NP1 and NP3 induce significant less to no toxicity compared to PS-COOH. Yet, despite enhanced deposition as well as increased uptake in HUVECs, PS-COOH are still non-toxic.

## Authors Contributions

L.-C. S. H., D. L., and C. H. performed organic, macromolecular, and colloidal synthesis and characterization.
I.-L. H. and S. F-D. performed the biological study.
S.-C. H. and J.-K. C. assisted on boron content evaluation.
L.-C. S. H. and G. D. conceived the project.
L.-C. S. H., J. R. H., C. W., M.-H. H., and G. D. acquired funding.
D. L., C. W., and G. D. supervised the project.
L.-C. S. H., D. L., I.-L. H., C. W., and G. D. wrote the paper.
All authors approved the submitted version.

## References


1 S. R. Mane, I. L. Hsiao, M. Takamiya, D. Le, U. Straehle, C. Barner-Kowollik, C. Weiss and G. Delaittre, *Small*, 2018, **14**, 1801571.
2 G. M. DeLoid, J. M. Cohen, G. Pyrgiotakis, S. V. Pirela, A. Pal, J. Liu, J. Srebric and P. Demokritou, *Part. Fibre Toxicol.*, 2015, **12**, 32.
3 I. Hansjosten, J. Rapp, L. Reiner, R. Vatter, S. Fritsch-Decker, R. Peravali, T. Palosaari, E. Joossens, K. Gerloff, P. Macko, M. Whelan, D. Gilliland, I. Ojea-Jimenez, M. P. Monopoli, L. Rocks, D. Garry, K. Dawson, P. J. F. Röttgermann, A. Murschhauser, J. O. Rädler, S. V. Y. Tang, P. Gooden, M. F. A. Belinga-Desaunay, A. O. Khan, S. Briffa, E. Guggenheim, A. Papadiamantis, I. Lynch, E. Valsami-Jones, S. Diabaté and C. Weiss, *Arch. Toxicol.*, 2018, **92**, 633–649.